Dementia

The main clinical purpose of imaging in the setting of dementia has been and continues to be the identification of treatable structural disease. However, as the population ages, growing interest centers on understanding, characterizing, and potentially treating dementing illnesses. Although several types of imaging are applied, MRI is the most useful structural imaging modality. In this unit, specific protocols intended to maximize the contribution of MRI to the clinical evaluation of dementia are presented. Each protocol has, as its foundation, a whole brain screen designed to evaluate for treatable causes of dementia. Reflecting the frequent overlap of vascular disease with dementing illness, the screening protocol also serves as an optimal evaluation of the patient with suspected vascular dementia. Additional sequences or modifications are then used to answer specific clinical questions. The evaluation of normal pressure hydrocephalus is reserved for a later unit devoted to cerebrospinal fluid (CSF)-flow related diagnoses. The parameters given here are derived from experience at 1.5 vT and may need to be altered slightly depending on the field strength and the equipment manufacturer.

VASCULAR DEMENTIA

BASIC PROTOCOL 1

Evaluation for usual structural treatable causes of dementia is not a demanding imaging problem. Indeed, one might argue that computed tomography (CT) would suffice for most applications. However, even a limited and fairly brief MR study will better characterize potential abnormalities and allow more sensitive detection of subtle lesions, such as subcortical ischemic injury, which is common in this patient group and may be of clinical consequence. Multiplanar imaging and improved sensitivity to blood products are additional advantages provided by MRI.

Table A5.3.1 lists the five sequences that comprise the basic screening protocol along with five additional sequences used to address specific imaging issues. Table A5.3.2 lists the hardware necessary to perform the procedure. Next, stepwise instructions for performing

Table A5.3.1 Screening Protocol/Vascular Dementia[a]

Type of weighting and sequence	Imaging plane
1. Pilot scan (scout)	—
2. T_1-weighted spin echo	Sagittal
3. T_2-weighted TSE/FSE	Transverse
4. Fast FLAIR	Transverse
5. T_2*-weighted gradient echo	Coronal
Additional sequences for specific dementia diagnoses:	
Alzheimer's evaluation	
6. 3-D short T_R T_1-weighted gradient echo	Oblique coronal
or	
7. T_1-weighted spin echo	Oblique coronal
Huntington's evaluation	
8. 3-D short T_R T_1-weighted gradient echo	Coronal
or	
9. T_1-weighted spin echo	Coronal
Parkinson's evaluation	
10. Dual echo PD-weighted/T_2-weighted CSE	Transverse

[a]Abbreviations: TSE, turbo spin echo; FSE, fast-spin echo; FLAIR, fluid attenuated inversion recovery; PD, proton density; CSE, conventional spin echo.

Contributed by Danial K. Hallam and Noriko Salamon-Muramaya
Current Protocols in Magnetic Resonance Imaging (2002) A5.3.1-A5.3.18

Table A5.3.2 Equipment Parameters

Coil type	Quadrature head coil
Gradient coil strength	25 mT/m or whatever the system permits
Cardiac gating	No
Peripheral gating	For safety only
Respiratory gating	No
Respirator	If required by patient
Oxygen	If required by patient
Motion cushions	Useful

the protocol are provided. The protocol is not terribly demanding of scanner hardware and may be performed on any clinical system. Basic Protocol 1 generally requires 20 to 25 min.

Set up patient and equipment

1. Interview the patient to ensure that he or she has no contraindications such as cardiac pacemakers or other implants containing ferromagnetic materials. Also be sure to find out if the patient has any health conditions that may require the presence of special emergency equipment or other precautions during the scanning procedure.

   In general, standard screening forms are used for all patients scanned in a magnetic resonance system (APPENDIX 1).

   The presence of any ferromagnetic metals may be a health hazard to the patient when he or she is inside the magnet, and will also affect the imaging. If in doubt as to the exact composition of the items, it is best to exclude patients with any metal implants; see Shellock and Kanal (1996) for a discussion of what implants may be safely scanned using magnetic resonance.

   Patients may be accompanied into the magnet room by a friend or family member, who can sit in the room during the scan and comfort the patient as needed. This companion must be screened as well to ensure the absence of loose metal objects on the body or clothing.

2. If the procedure is a research protocol, have the patient sign any necessary consent forms.
3. Have the patient remove all jewelry and change into a gown to eliminate any metal that might be found in clothing.
4. Have the patient wash off mascara or other makeup to avoid local tissue heating and image artifacts.
5. Inform the patient about what will occur during the procedure, what he or she will experience while in the magnet, and how to behave, including the following:
   a. If earphones or headphones are used to protect the ears from the loud sounds produced by the gradients, the patient will be asked to wear these, but will be able to communicate with you at any time during the imaging.
   b. The patient will be given a safety squeeze-bulb or similar equipment to request assistance at any time (demonstrate how this works).
   c. For good results, the patient should be instructed not to talk unless absolutely necessary and to avoid or minimize swallowing and other movements during each scan—i.e., as long as the banging sounds continue. Between scans, talking and swallowing are acceptable in most cases, but should be avoided when comparative positional studies are being performed; the patient will be informed when this is the case.
   d. Nevertheless, the patient may call out at any time if he or she feels it necessary.

6. Have the patient lie onto the table. Set up any triggering devices or other monitoring equipment that is to be used either before or just after the patient lies down.
7. Center the patient in the head coil. Make sure that the head and neck are constrained to limit motion.

   Generally, the patient's head is fixed so that the head is horizontal (not tilted) and the neck and head lie along the axis of the patient table; other positions may be appropriate depending on the needs at hand.
8. If needed, place a pillow or other support under the knees to make the patient more comfortable.
9. Use the centering light to position the patient's nasion and put him or her into the center of the magnet.

   Once this step has been performed, so long as the patient does not move on the table, the table itself can be moved and then replaced in the same position as before without jeopardizing the positioning of one scan relative to another.
10. If the patient is unable to hold still, provide an appropriate sedative.

Sequence 1: Rapid three-plane positioning pilot

11. To validate the patient's position, run the system's pilot (or scout) scan to ensure correct location of the head in three dimensions, using the imaging sequence given in Table A5.3.3 or similar parameters.

    This sequence usually consists of three orthogonal planes to allow localization. The images are often also used later to determine where to place the saturation pulses and to set up total coverage of the volume of interest.

    If the pilot scan shows the patient's head to be significantly off-center then it may be helpful to reposition the patient and repeat the pilot scan.

Sequence 2: Sagittal T_1-weighted spin echo

12. Using images generated in sequence 1, plan sagittal images to provide whole brain coverage. Set the parameters as indicated in Table A5.3.4. Run sequence 2.

    The scan is best positioned first on the transverse pilot scan. Some angulation may be needed to provide for true sagittal anatomic imaging. The coverage provided should then be checked on the sagittal scout. This sequence is used to accurately position subsequent scans. It provides excellent visualization of midline structures.

Sequence 3: Transverse T_2-weighted TSE/FSE

13. Use the sagittal T_1-weighted image to position transverse scans. Set parameters as given in Table A5.3.5. Run sequence 3.

    The scan is positioned graphically to provide whole brain coverage. The slices should be angled according to an institutional standard for transverse images. The authors recommend using the "AC-PC" line as such a standard. See Figure A5.1.2. Here, the anterior and posterior commissures are identified on the sagittal T_1-weighted midline image. The slices of all transverse scans are positioned parallel to a line drawn between the two landmarks. The sequence provides excellent visualization of the whole brain.

Sequence 4: Transverse fast FLAIR

14. Set parameters for transverse fast FLAIR as indicated in Table A5.3.6. Run sequence 4.

    The scan is positioned identically to sequence 3. The sequence provides superior demonstration of T_2-weighted bright lesions, especially in the supratentorial compartment. The suppression of bright CSF afforded by the FLAIR technique demonstrates lesions adjacent to CSF that would otherwise be poorly visualized. Subtle subcortical ischemic injury is optimally visualized. FLAIR also nicely demonstrates extra-axial fluid collections, such as subdural hematomas, occasionally seen in this patient population.

Table A5.3.3 Parameters for Pilot Scan (Scout)

Patient position	Supine
Scan type	Gradient echo
Imaging plane (orientation)	3 planes
Central slice or volume center	Run initially at magnet isocenter
Echo time (T_E)	Minimum
Repeat time (T_R)	Minimum
Flip angle (FA)	20°
Fields of view (FOV_x, FOV_y)	300 mm, 300 mm
Resolution (Δx, Δy)	1.17 mm, 1.56 mm
Number of data points collected (N_x, N_y)	256, 192
Display matrix (D_x, D_y)	256, 256
Slice thickness (Δz)	5 mm
Number of slices	3, one in each of 3 cardinal planes
Slice gap	Not applicable
Number of acquisitions (N_{acq})	1
Swap read and phase encoding	No
Scan time	~10 sec

Table A5.3.4 Parameters for Sagittal T_1-Weighted Spin Echo

Patient position	Supine
Scan type	Spin echo
Imaging plane (orientation)	Sagittal
Central slice or volume center	Midline
Echo time (T_E)	14 msec
Repeat time (T_R)	600 msec
Flip angle (FA)	90°
Fields of view (FOV_x, FOV_y)	230 mm, 230 mm
Resolution (Δx, Δy)	1.20 mm, 0.90 mm
Number of data points collected (N_x, N_y)	192, 256
Slice thickness (Δz)	5 mm
Number of slices	19–21
Slice gap (distance factor)	1.5 mm (0.30)
Number of acquisitions (N_{acq})	1
Read direction	Cranio-caudal
Saturation pulses	Inferior may be used
Scan time	~2 min

Sequence 5: Coronal T_2^*-weighted gradient echo

15. Set parameters as indicated in Table A5.3.7. Using sagittal T_1-weighted images, position coronal images orthogonal to transverse images using graphic prescription for whole brain coverage. Run sequence 5.

This sequence is designed to provide sensitivity to blood products through exploitation of their susceptibility effects. Punctate foci of hemorrhage as seen in amyloid angiopathy or coating of brain surfaces with hemosiderin as seen in superficial siderosis may not be detected without susceptibility weighting. Use of the coronal plane simplifies interpretation of skull base susceptibility artifacts inherent to this sequence.

Table A5.3.5 Parameters for Transverse T_2-Weighted TSE/FSE

Patient position	Supine
Scan type	TSE/FSE
Imaging plane (orientation)	Transverse
Central slice or volume center	Position for whole brain coverage
Echo time (T_E)	85 msec
Echo train length (ETL)	5 to 8
Repeat time (T_R)	2500 to 3000 msec
Flip angle (FA)	90°
Fields of view(FOV_x, FOV_y)	180 mm, 230 mm
Resolution (Δx, Δy)	0.94 mm, 0.90 mm
Number of data points collected (N_x, N_y)	192, 256
Slice thickness (Δz)	5 mm
Number of slices	23
Slice gap (distance factor)	1.5 mm (0.30)
Number of acquisitions (N_{acq})	1–2
Read direction	Anterior to posterior
Saturation pulses	Inferior may be used
Scan time	~1–4 min

Table A5.3.6 Parameters for Transverse Fast FLAIR

Patient position	Supine
Scan type	Fast FLAIR
Imaging plane (orientation)	Transverse
Central slice or volume center	Position for whole brain coverage
Echo time (T_E)	105–140 msec[a]
Echo train length (ETL)	7–11
Repeat time (T_R)	8000–10,000 msec[a]
Inversion time (T_I)	2000–2400 msec[a]
Flip angle (FA)	180°
Fields of view (FOV_x, FOV_y)	180 mm, 230 mm
Resolution (Δx, Δy)	0.94 mm, 0.90 mm
Number of data points collected (N_x, N_y)	192, 256
Slice thickness (Δz)	5 mm
Number of slices	23
Slice gap (distance factor)	1.5 mm (0.3)
Number of acquisitions (N_{acq})	1
Read direction	Anterior to posterior
Saturation pulses	Inferior may be used
Scan time	~2.5–5 min

[a]Optimum choice of parameters for fast FLAIR varies significantly with manufacturer and scanner limitations. For a review of parameter optimization in fast FLAIR, please refer to Rydberg et al. (1995).

Table A5.3.7 Parameters for Coronal T_2^*-Weighted Gradient Echo

Patient position	Supine
Scan type	2-D gradient echo
Imaging plane (orientation)	Coronal
Central slice or volume center	Position for whole brain coverage
Echo time (T_E)	20–25 msec
Repeat time (T_R)	600–900 msec[a]
Flip angle (FA)	20°
Fields of view (FOV_x, FOV_y)	180 mm, 230 mm
Resolution (Δx, Δy)	0.94 mm, 0.90 mm
Number of data points collected (N_x, N_y)	192, 256
Slice thickness (Δz)	4–6 mm
Number of slices	19–21
Slice gap	1–2 mm
Number of acquisitions (N_{acq})	1–2
Read direction	Cranio-caudal
Saturation pulses	Inferior may be used
Scan time	~2–6 min

[a]Manufacturers vary in the efficiency of multiplanar slice acquisition in this sequence. Choice of T_R and slice thickness amounts to a trade-off between imaging time and resolution.

BASIC PROTOCOL 2

ALZHEIMER'S DISEASE

Routine MRI scans nicely depict atrophy of mesial temporal lobe structures that suffer the dominant impact of Alzheimer-type degenerative changes. In this protocol, an angled T_1-weighted sequence to provide a cross-section of hippocampal structures is chosen to demonstrate these changes (Fig. A5.3.1). Multiple investigators employ a 3-D, short T_R, T_1-weighted gradient echo sequence for sophisticated volumetric studies on Alzheimer disease (AD) patients. Such a sequence is recommended in addition to the screening protocol (see Basic Protocol 1) as an AD focused exam. Alternatively, a coronal T_1-weighted spin echo sequence will suffice when visual inspection only is planned. Compared to the 3-D volume sequence, the 2-D spin echo sequence has the advantages of being somewhat shorter in duration and overall less vulnerable to motion degradation.

Set up patient and equipment

1. Use the same equipment and perform patient setup as in Basic Protocol 1, steps 1 to 10.
2. Perform sequences 1 to 5 as described in Basic Protocol 1.

Sequence 6: Additional sequence for AD: 3-D oblique coronal short T_R T_1-weighted gradient echo

3. Set parameters as indicated in Table A5.3.8. The scan is positioned graphically by first locating the hippocampus on an off-midline slice from the sagittal T_1-weighted sequence (Fig. A5.3.2). Then position the volume for the current sequence so that the plane of acquisition is orthogonal to the axis of the hippocampus. If the hippocampus proves difficult to identify, then as a fall back approach, one may position the scan to be parallel to the axis of the brainstem—this is usually a very similar plane as that chosen directly orthogonal to the axis of the hippocampus. Run sequence 6.

   This sequence demonstrates anatomy of mesial temporal lobe structures allowing for optimal identification of the disproportionate atrophy seen in AD. The 3-D technique employed provides thin slices and allows for reformations in additional planes.

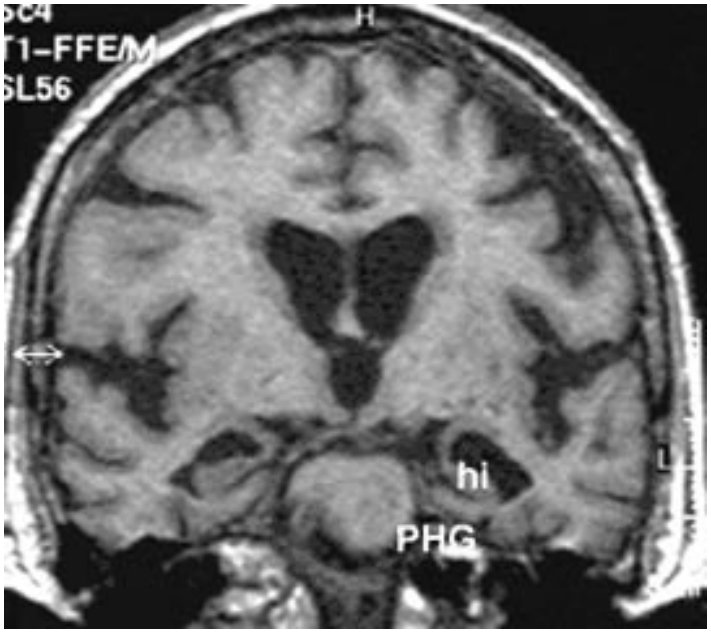

Figure A5.3.1 A coronal T_1-weighted image demonstrates disproportionate atrophy of mesial temporal lobe structures, most notably the hippocampus (hi). Parahippocampal gyrus is also marked (PHG).

Table A5.3.8 Parameters for Sequence 6: 3-D Oblique Coronal T_1-Weighted

Patient position	Supine
Scan type	3-D gradient echo
Imaging plane (orientation)	Oblique coronal
Pulse sequence database	SPGR
Central slice or volume center	Temporal lobe
Echo time (T_E)	"Minimum full" (~6 msec)
Repeat time (T_R)	33 msec
Flip angle (FA)	35°–45°
Fields of view (FOV_x, FOV_y)	165 mm, 220 mm
Resolution (Δx, Δy)	1.15 mm–0.86 mm, 0.86 mm
Number of data points collected (N_x, N_y)	144–192, 256
Slice thickness (Δz)	1.61 mm
Number of slices	124
Slab thickness	200 mm
Slice gap	0 mm
Number of acquisitions (N_{acq})	0.75[a]
Read direction	Cranio-caudal (superior to inferior)
Saturation pulses	Inferior may be used
Scan time	7.5–10 min

[a]Refers to ¾-NEX imaging, also known as partial Fourier imaging—an option available on many clinical scanners. Partial Fourier imaging reduces imaging time by exploiting the inherent symmetry of *k*-space; essentially, fewer phase encoding steps are used to provide the same spatial resolution. The time saved is at the expense of the signal-to-noise ratio.

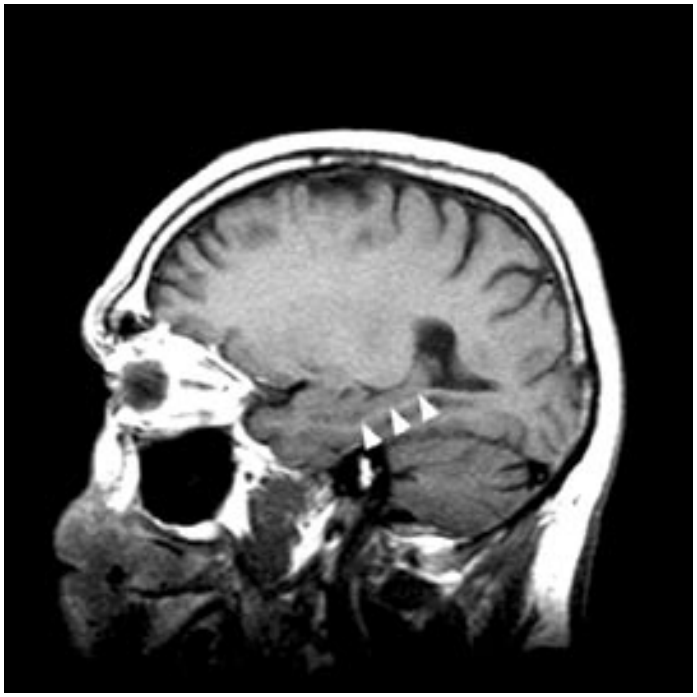

Figure A5.3.2 An off-midline sagittal T_1-weighted image allows visualization of long axis of hippocampus (along arrowheads). Oblique coronal T_1-weighted images are positioned perpendicular to the hippocampal long axis.

Table A5.3.9 Parameters for Oblique Coronal T_1-Weighted Spin Echo

Patient position	Supine
Scan type	Spin echo
Imaging plane (orientation)	Oblique coronal
Central slice or volume center	Position for whole brain coverage
Echo time (T_E)	14 msec
Repeat time (T_R)	600 msec
Flip angle (FA)	90°
Fields of view (FOV_x, FOV_y)	180 mm, 230 mm
Resolution (Δx, Δy)	0.94 mm, 0.90 mm
Number of data points collected (N_x, N_y)	192, 256
Slice thickness (Δz)	5 mm
Number of slices	23
Slice gap (distance factor)	1.5 mm (0.30)
Number of acquisitions (N_{acq})	1–2
Read direction	Superior to inferior
Saturation pulses	Inferior may be used
Scan time	~2–4 min

Sequence 7: Alternate additional sequence for AD: 2-D oblique coronal T_1-weighted spin echo

4. Set parameters as indicated in Table A5.3.9. The scan is positioned in a manner identical to that described for sequence 6. Run sequence 7.

   This sequence demonstrates anatomy of mesial temporal lobe structures allowing for optimal identification of the disproportionate atrophy seen in AD.

HUNTINGTON'S DISEASE

BASIC PROTOCOL 3

Characteristic pathologic abnormalities for Huntington's disease consist of bilateral atrophy of the caudate nucleus and putamen (together denoted striatum), often accompanied by a moderate degree of gyral atrophy in the frontal and temporal regions. The striatal atrophy is best demonstrated in coronal plane (Fig. A5.3.3). As with Alzheimer's disease, a coronal T_1-weighted sequence is chosen for its superior demonstration of anatomy. Unlike the AD evaluation, the sequence is positioned in routine coronal and not oblique coronal orientation. Again, an option of 3-D, short T_R, T_1-weighted gradient echo or 2-D T_1-weighted spin echo is provided. Considerations regarding sequence choice are identical to those noted in Basic Protocol 2.

Set up patient and equipment

1. Use the same equipment and perform patient setup as in Basic Protocol 1, steps 1 to 10.
2. Perform sequences 1 to 5 as described previously.

Sequence 8: Additional sequence for Huntington's disease: 3-D coronal short T_R T_1-weighted gradient echo

3. Set parameters as indicated in Table A5.3.8 with orientation to be normal coronal. The scan is positioned perpendicular to prior transverse sequences (sequences 3 and 4). Run sequence 8.

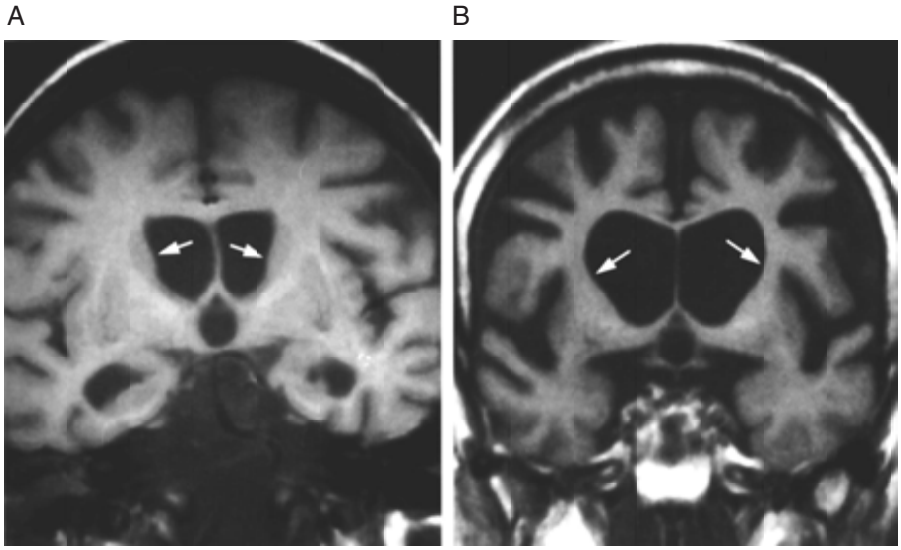

Figure A5.3.3 Coronal T_1-weighted images of two Huntington's patients, (A) and (B), demonstrating caudatal atrophy seen with advanced disease. In the normal, the caudate head bulges into the lateral aspect of the anterior horn of the lateral ventricles. Atrophy of the caudate head results in loss of the usual medially oriented convex margin, which may become flattened or with increasing atrophy, concave. Reproduced from D.H. Yock (1995) with permission from Mosby.

Sequence 9: Alternate additional sequence for Huntington's disease: 2-D coronal T_1-weighted spin echo

4. Set parameters as indicated in Table A5.3.9 with orientation to be normal coronal. The scan is positioned perpendicularly to prior transverse sequences (sequences 3 and 4). Run sequence 9.

BASIC PROTOCOL 4

PARKINSON'S DISEASE

Little in the way of structural abnormality is present in Parkinson's disease. However, subtle findings in the midbrain reflecting the loss of dopaminergic nigrostriatal neurons from the pars compacta of the substantia nigra have been identified (Duguid et al., 1986; Rutledge et al., 1987; Braffman et al., 1989; Olanow, 1992). These findings consist of narrowing or smudging of the high signal regions separating the substantia nigra from the red nucleus and are best demonstrated by a sequence providing some susceptibility weighting (Fig. A5.3.4). A conventional dual echo PD-weighted/T_2-weighted spin echo sequence is chosen for this application.

Set up patient and equipment

1. Use the same equipment and perform equipment and patient setup as in Basic Protocol 1, steps 1 to 10.

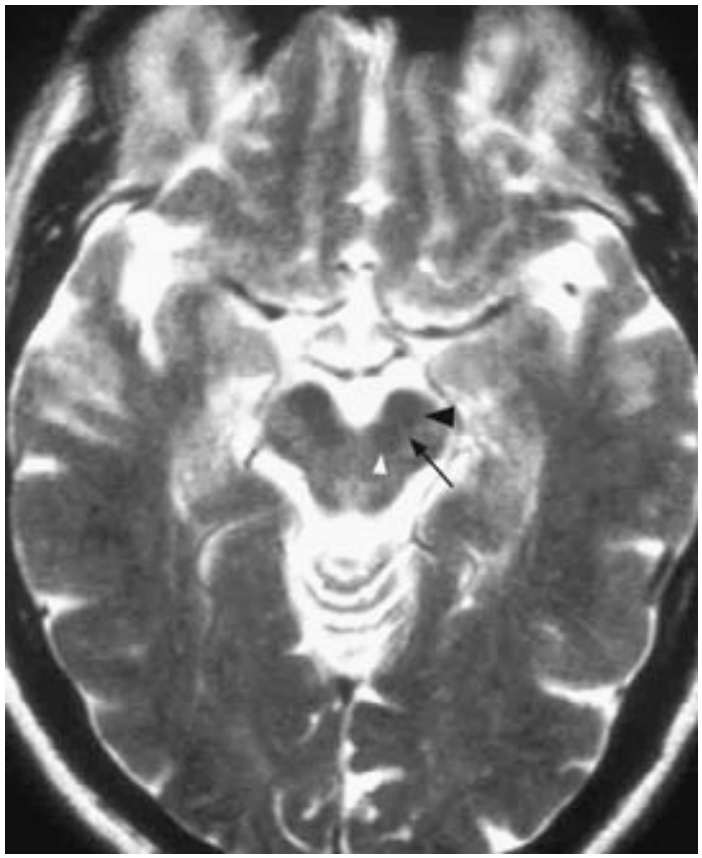

Figure A5.3.4 Conventional T_2-weighted spin echo demonstrates narrowing and smudging of pars compacta (arrow) in Parkinson's Disease. The pars reticulata (black arrowhead) of the substantia nigra exhibits low signal secondary to mineralization. The red nucleus (white arrowhead) is similarly recognized.

Table A5.3.10 Parameters for Dual Echo PD-Weighted/T_2-Weighted Conventional Spin Echo

Patient position	Supine
Scan type	Conventional spin echo
Imaging plane (orientation)	Transverse
Central slice or volume center	Midbrain
Echo time (T_E)	30 msec and 80 msec
Repeat time (T_R)	2500 msec
Flip angle (FA)	90°
Fields of view (FOV_x, FOV_y)	180 mm, 230 mm
Resolution (Δx, Δy)	0.94 mm, 0.90 mm
Number of data points collected (N_x, N_y)	192, 256
Slice thickness (Δz)	5 mm
Number of slices	20
Slice gap (distance factor)	1–1.5 mm (0.20–0.30)
Number of acquisitions (N_{acq})	0.75[a]
Read direction	Anterior to posterior
Saturation pulses	Inferior may be used
Scan time	~6 min

[a]Refers to ¾NEX imaging, also known as partial Fourier imaging—an option available on many clinical scanners. Partial Fourier imaging reduces imaging time by exploiting the inherent symmetry of *k*-space; essentially, fewer phase encoding steps are used to provide the same spatial resolution. The time saved is at the expense of the signal-to-noise ratio.

2. Perform sequences 1 to 5 as described previously. The transverse T_2-weighted sequence TSE may be omitted to save time.

Sequence 10: Additional sequence for Parkinson's disease: Transverse dual echo PD-weighted/T_2-weighted spin echo

3. Set parameters as indicated in Table A5.3.10. The scan is positioned in the routine transverse plane—as done for sequence 3. Run sequence 10.

The sequence will require more scanning time than the FSE/TSE sequence. With the T_2-weighted coverage provided, the T_2-weighted TSE becomes somewhat redundant and may be omitted. A conventional spin echo sequence is chosen because it provides modest susceptibility weighting allowing visualization of mineralizated areas of the substantia nigra. A more heavily gradient echo sequence may result in some "blooming" of the iron, thereby obscuring the adjacent high signal region whose narrowing is detected. Sequences minimizing susceptibility effect (FSE/TSE) might suffice, however, their utility for this application has not been documented in the literature.

COMMENTARY

Background Information

Expected marked increases in the number of elderly magnify the need for improved evaluation, understanding, and, if possible, treatment of dementia. The world population >65 years of age is anticipated to grow at an annual rate of 2.4%, leading to estimates of 37 million demented people worldwide by the year 2020 (Cooper, 1994). In the U.S., ~5% of the population >65 years of age has severe dementia with estimates of ≥15% for the population >85 years (Evans et al., 1989). Alzheimer's disease is the most common cause of dementia accounting for over one half of all cases. Its financial cost in the U.S. has been estimated at 60 billion dollars annually (Adams et al., 1997). In one series, the Alzheimer's incidence rate was 123 cases per 100,000 yearly (Schoenberg et al., 1987). Prevalence increases drastically with age. Per 100,000 population, prevalence is 3200 in ages 70 to 79 years and 10,800 in individuals >80 years (Adams et al., 1997).

Routine clinical imaging of demented patients may not be necessary depending on the clinician's level of confidence in the diagnosis. In general practice, any uncertainty regarding the diagnosis usually prompts performance of either CT or MRI. Imaging is specifically recommended when focal signs or symptoms suggest either underlying treatable disorder (e.g., subdural hematoma, hydrocephalus, tumor) or the presence of co-existent pathology (e.g., stroke, hemorrhage; Larson et al., 1986; Hollister and Boutros, 1991). Imaging is also recommended in the setting of acute onset or rapid progression of dementia symptoms.

In the following, an attempt to present a complete discussion of the imaging findings in dementia will not be made. Rather, specific imaging findings relevant to protocol issues will be emphasized. For the interested reader, several recent excellent reviews of neuroimaging in dementia are available, including discussions representing radiologic (Braffman, 2000) and neurologic (Chawluk, 1999) perspectives.

Alzheimer's disease

The gross pathologic appearance in AD consists of variable atrophy of temporal, frontal, and parietal lobes with some sparing of perirolandic regions. In the past decade, much interest has centered on use of quantitative MRI techniques to measure volume of hippocampi and other mesial temporal lobe (MTL) structures. The interest in this specific region derives from several observations. First, atrophy of MTL structures has been observed early and more extensively in AD patients (de Leon et al., 1989). Second, recognizing the central role of MTL structures in memory (Squire, 1992), memory impairment is an early and severe manifestation of AD. Finally, the anatomy of this particular region lends itself to volumetric analysis more readily than that of other AD involved structures.

Techniques applied to evaluation of MTL atrophy in AD range from visual inspection to sophisticated volumetric quantification. Somewhat surprisingly, even simple visual inspection has some utility and has been shown to support the diagnosis of AD (sensitivity 81%; specificity 67%) versus control population, especially in groups with lower baseline atrophy (subjects <75 years of age; Scheltens et al., 1992). Barclay and colleagues (1992) applied subjective evaluation of MRI to distinguish patients with AD from those with multi-infarct dementia or mixed diagnostic features yielding reasonable specificity in diagnosing AD. Frisoni applied a series of linear measurements relating to MTL structures in a group of patients with mild to moderate AD (Frisoni et al., 1996). A compound measure including temporal horn and choroid fissure widths along with hippocampal height was 86% sensitive in discriminating patients with mild AD from controls. As a logical next step, Jack et al. applied volumetric measurement of MTL structures in an effort to diagnose patients with the mildest form of AD as indicated by Clinical Dementia Rating scores (Jack et al., 1997). Volume measurements of hippocampi were 72% sensitive (with specificity 90%) in diagnosing patients with very mild AD compared with controls.

More recent studies have attempted to identify individuals at risk for developing AD using MTL atrophy measurements. Convit and colleagues studied patients with minimal cognitive impairment (MCI), a clinically defined group with mild memory and/or word finding deficiency, 75% of whom progress eventually to AD (Flicker et al., 1991; Convit et al., 1997). Hippocampal volume measurements correctly classified MCI subjects compared with normals 74% of the time. Similar results supporting the ability of hippocampal volume estimates to identify individuals at risk for AD have been published by other laboratories (Kaye et al., 1997; Jack et al., 1999).

Huntington's disease

Huntington's disease (HD) is readily recognized by the clinical triad of chorea, dementia, and personality disorder along with family history reflecting its dominant inheritance pattern. In questionable cases, genetic analysis is used to identify the defective gene. Such evaluation may even be applied in asymptomatic patients. For this reason, imaging evaluation is now rarely utilized in most centers.

Characteristic imaging findings have been described that are quite apparent in advanced cases (Fig. A5.3.3). Directly paralleling the pathologic changes, imaging demonstrates pronounced bilateral atrophy of the caudate and putamen (Simmons et al., 1986). The caudatal atrophy results in a characteristic loss of the usual bulge of caudate head into the anterior horn of the lateral ventricle. On MRI, signal abnormalities have been described in the striatum and may consist variably of either decrease or increase in signal intensity (Savoiardo et al., 1991). Diffuse cerebral atrophy, especially of the frontal lobes, occurs in later

stages of HD and correlates with cognitive decline (Starkstein et al., 1992; Aylward et al., 1998).

Volumetric techniques are useful in mild cases and might potentially have some value in monitoring response to therapy. Atrophy of the putamen, as demonstrated by MRI, exceeds that of the caudate in mild disease (Harris et al., 1992). Decreased basal ganglia volume has been shown to correlate with presence of the gene for HD in asymptomatic subjects (Aylward et al., 1994). Additionally, greater rate of basal ganglia atrophy has been shown to correlate with earlier symptom onset (Aylward et al., 1997).

Parkinson's disease

The diagnosis of Parkinson's disease rests on clinical observation including core findings of expressionless face, paucity of voluntary movement, and resting tremor among others. On MRI, reflecting the pathologic hallmark of loss of pigmented cells in the substantia nigra, especially in the pars compacta, the width of the pars compacta is narrowed relative to controls (Fig. A5.3.4; Duguid et al., 1986). The observed narrowing of the pars compacta presumably relates to neuronal loss or may otherwise reflect iron deposition.

The diagnostic challenge in Parkinson's disease is generally one of separating it from numerous other Parkinsonian syndromes, including progressive supranuclear palsy, corticobasal degeneration and the various forms of multiple system atrophy. Occasionally, imaging may be helpful in this regard. It should first be noted that the finding on proton density weighted images of pars compacta narrowing is not useful in this regard as it has been reported in other Parkinsonian syndromes including striatonigral degeneration and progressive supranuclear palsy (Stern et al., 1989). Separate findings for the specific Parkinsonian syndromes are occasionally observed and may be useful. In progressive supranuclear palsy (PSP), some, but not all, patients exhibit focal atrophy/signal abnormality of superior colliculi and/or periadequeductal regions (Fig. A5.3.5; Savoiardo et al., 1989), a finding not seen in typical Parkinson's patients. The diagnosis of PSP can be confused with that of corticobasal degeneration (CBD), especially at disease onset because atypical presentations are not uncommon and the clinical syndromes may be incompletely expressed (Davis et al., 1985; Bergeron et al., 1996). Soliveri and colleagues reviewed the cognitive and MRI findings of these two clinically overlapping illnesses. They found the MRI findings of midbrain atrophy in PSP and asymmetric frontoparietal atrophy in CBD to be the most useful and consistent aids to clinical evaluation in distinguishing the two diseases (Soliveri et al., 1999).

The term multiple system atrophy refers to the complex syndrome exhibiting various degrees of Parkinsonism (striatonigral degeneration), ataxia (olivopontocerebellar degeneration), and autonomic dysfunction (Shy-Drager syndrome). Each of these disorders may occur either in isolation or in combination. Nearly all forms of multiple system atrophy exhibit focal low T_2-weighted signal in the putamen, described as "slit-like" signal void (Fig. A5.3.6; Savoiardo et al., 1989; Lang et al., 1994). The signal loss is presumed due to iron deposition related to neuronal degeneration and is best demonstrated with the susceptibility weighting afforded by a T_2^*-weighted gradient echo sequence. Signal loss in the putamen distinguishes patients with multiple system atrophy from those with typical Parkinson's disease and age-matched controls (Olanow, 1992). Olivopontocerebellar degeneration is characterized by marked neuronal loss in inferior olives, pons, and cerebellum. In advanced cases, inspection of T_1-weighted sagittal and T_2-weighted transverse images reveals marked atrophy of pons and cerbellar cortex, findings helpful in diagnosis (Fig. A5.3.7; Savoiardo et al., 1990).

Structural lesions of a variety of etiologies may result in a Parkinsonian syndrome. Toxic diseases resulting in focal basal ganglia lesions may be associated with Parkinsonism. Focal bilateral necrosis of the basal ganglia may result from carbon monoxide poisoning, cyanide poisoning, methanol intoxication, among others, and all may be associated with Parkinsonism (Ley and Gali, 1983; Carella et al., 1988; Messing and Storch, 1988; Verslegers et al., 1988; Rosenberg et al., 1989; Lee and Marsden, 1994; Choi and Cheon, 1999; Sohn et al., 2000). Metabolic disorders resulting in dense basal ganglia calcification such as hypoparathyroidism and pseudohypoparathyroidism may be associated with various movement disorders related to compromised function of the calcified nuclei (Pearson et al., 1981). Parkinsonism may be an unusual manifestation of hydrocephalus including both obstructive causes and as a component of normal pressure hydrocephalus (Miodrag et al., 1987; Curran and

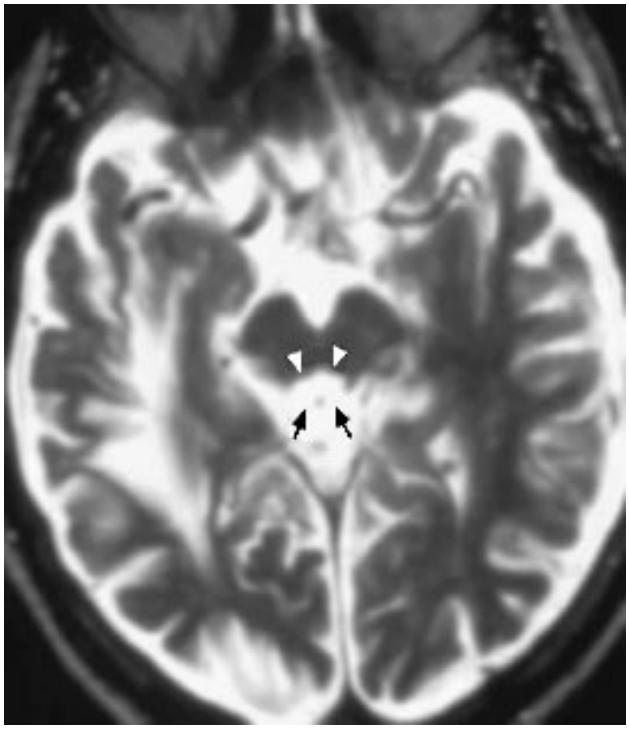

Figure A5.3.5 Patient with progressive supranuclear palsy. Characteristic focal marked atrophy of the superior colliculi (black arrows) and periaqueductal region (white arrowheads) is present.

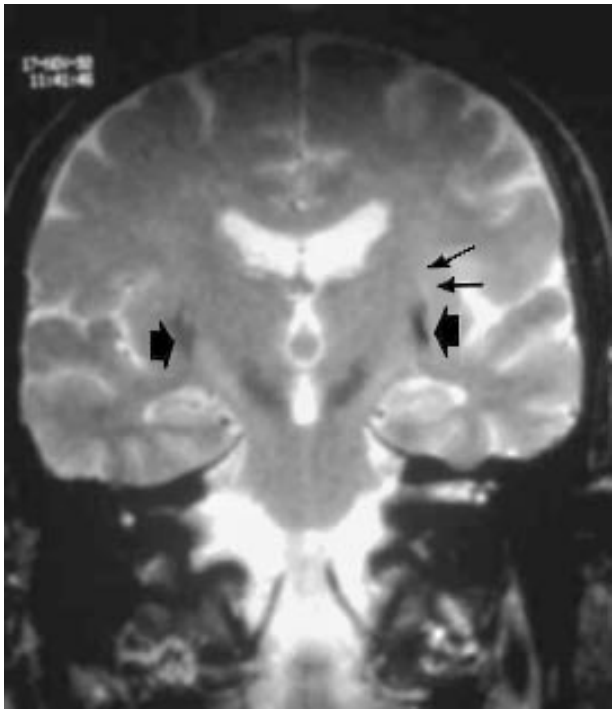

Figure A5.3.6 Patient with striatonigral degeneration. T_2-weighted coronal image demonstrates slit-like signal void in putamen (large arrows) resulting from iron depostion. In this case, some high signal was also seen adjacent to the patient's left putamen (small arrows).

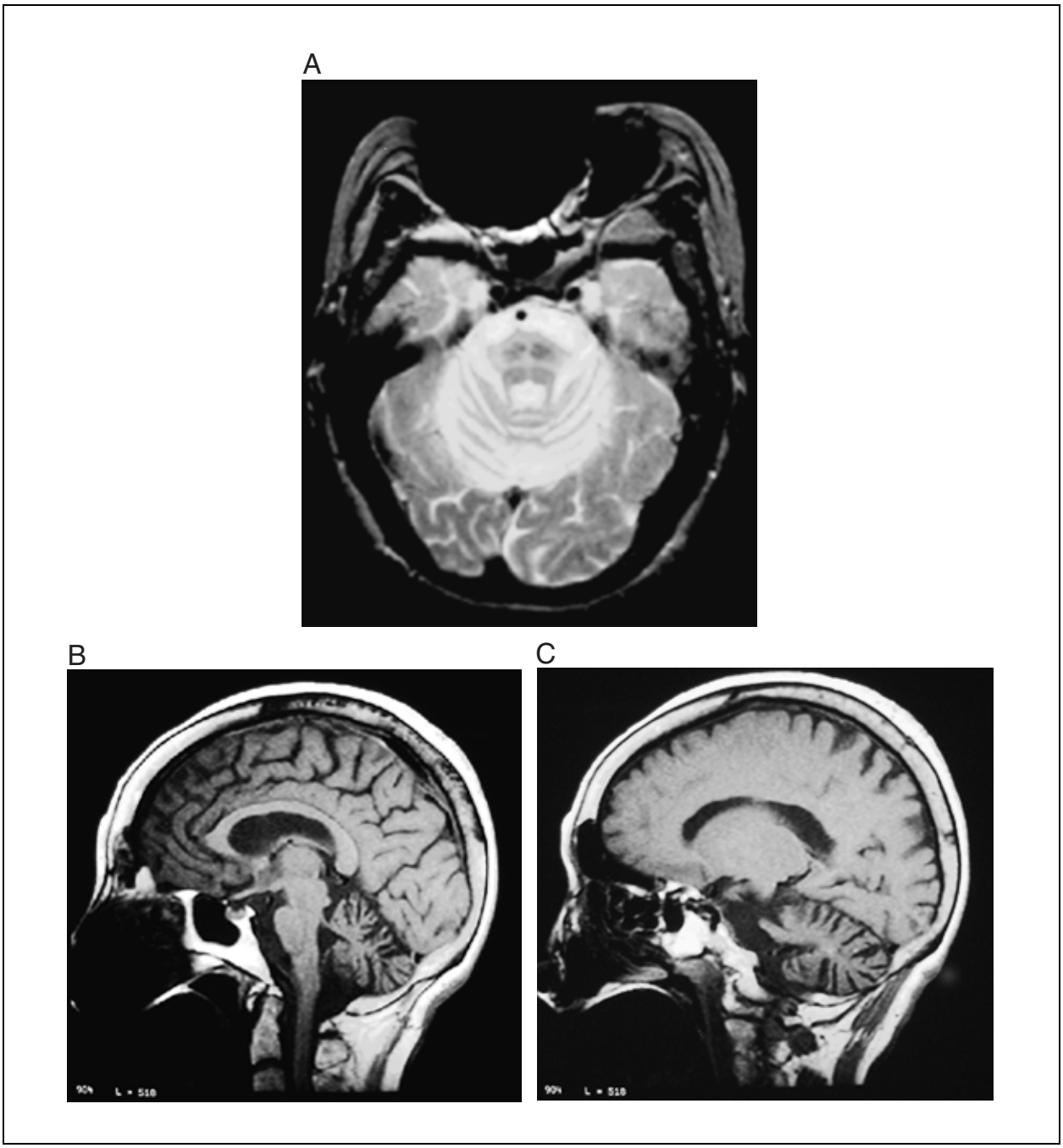

Figure A5.3.7 Profound atrophy of pons and cerebellum demonstrated by T_2-weighted transverse (**A**) and T_1-weighted sagittal, midline (**B**) and para-midline (**C**) in this patient with olivopontocerebellar degeneration as a component of multiple system atrophy.

Lang, 1994; Friedman, 1996; Krauss et al., 1997). Even multiple deep grey infarcts may result in Parkinsonism (Zijlmans et al., 1995).

Critical Parameters and Troubleshooting

Motion artifacts may be a problem for nearly any MRI examination and can be particularly problematic in the population evaluated for dementia. As always, proper care in placing and securing the patient in the head coil is critical as is the interaction of the MRI technologist with the patient. In cases in which such measures are insufficient, prudent conscious sedation should be employed if at all possible. If sedation fails or is not possible, then faster imaging may be considered. As a first step, the provided sequences may be shortened simply by reducing the acquisition matrix (N_x, N_y). Fast imaging techniques do exist and will be described in a later unit. However, such techniques are particularly limited in matters of

contrast and so may poorly demonstrate subcortical ischemic injury and focal (especially deep gray matter) atrophy.

Proper contrast in fast FLAIR imaging is important to the dementia protocol. As noted previously, manufacturers vary in their implementation of this sequence, including the parameters employed. Utilization of FLAIR should begin with the manufacturer's standard parameters. Beyond this, some modifications may yield more appealing images with improved T_2-weighted lesion contrast. Use of a T_R that is too low (i.e., <7000 msec) compromises both T_2-weighted contrast and CSF suppression. The T_E should be fairly long, at least 100 msec, again for reasons related to T_2-weighted contrast. The inversion time (T_I) is dictated by the T_1 of CSF and for a 1.5-T magnet should be between 2200 and 2400 msec. The reader is referred to Rydberg et al. (1995) for a thorough discussion of the considerations involved.

The choice of T_E in the T_2^*-weighted sequence affects sensitivity to blood products. The use of a longer T_E allows more time for spin dephasing thereby enhancing detection of small areas of old blood. In some ways, this choice reflects a trade-off between increasing sensitivity to old blood and reducing distracting skull base susceptibility artifacts. The use of coronal plane for this sequence is designed to limit uncertainty in recognition of skull base artifacts. The recommended T_E range of 20 to 25 msec is empirically derived. Susceptibility effects are strongly related to magnetic field strength and are significantly decreased even at 1.0 T compared to 1.5 T. Use of longer T_E at lower field strengths will only partially compensate for the reduced susceptibility effect.

Anticipated Results

The exam should provide full imaging characterization of brain parenchymal lesions including cortical and subcortical infarctions, encephalomalacia, as well as diffuse and focal atrophy. To accomplish this end, several types of sequences with various T_1, T_2, and susceptibility weighting are employed, including T_1-weighted spin echo, fast FLAIR, T_2-weighted FSE or CSE, and T_2^*-weighted gradient echo. Each of these is performed in the plane in which it is most helpful. The coronal T_2^*-weighted gradient echo sequence optimally demonstrates the hemorrhagic nature of lesions and in doing so may illuminate the diagnosis. The addition of a sequence in the coronal plane better demonstrates the location of some lesions and is particularly helpful in characterizing encephalomalacia related to prior trauma.

Literature Cited

Adams, R.D., Victor, M., and Ropper, A.H. 1997. Principles of Neurology. McGraw-Hill, New York.

Aylward, E.H., Brandt, J., Codori, A.M., Mangus, R.S., Barta, P.E., and Harris, G.J. 1994. Reduced basal ganglia volume associated with the gene for Huntington's disease in asymptomatic at-risk persons. *Neurology* 44:823-828.

Aylward, E.H., Li, Q., Stine, O.C., Ranen, N., Sherr, M., Barta, P.E., Bylsma, F.W., Pearlson, G.D., and Ross, C.A. 1997. Longitudinal change in basal ganglia volume in patients with Huntington's disease. *Neurology* 48:394-399.

Aylward, E.H., Anderson, N.B., Bylsma, F.W., Wagster, M.V., Barta, P.E., Sherr, M., Feeney, J., Davis, A., Rosenblatt, A., Pearlson, G.D., and Ross, C.A. 1998. Frontal lobe volume in patients with Huntington's disease. *Neurology* 50:252-258.

Barclay, L.L., Linden, C., and Murtagh, R. 1992. Medial temporal atrophy as a magnetic resonance imaging marker for Alzheimer's disease. *J. Neuroimaging* 2:131-135.

Bergeron, C., Pollanen, M.S., Weyer, L., Black, S.E., and Lang, A.E. 1996. Unusual clinical presentations of cortical-basal ganglionic degeneration. *Ann. Neurol.* 40:893-900.

Braffman, B.H. 2000. The aging brain and neurodegenerative disorders. *In* Neuroimaging: Clinical and Physical Principles (R.A. Zimmerman, W.A. Gibby, and R.F. Carmody, eds.) pp. 951-978. Springer, New York.

Braffman, B.H., Grossman, R.I., Goldberg, H.I., Stern, M.B., Hurtig, H.I., Hackney, D.B., Bilaniuk, L.T., and Zimmerman, R.A. 1989. MR imaging of Parkinson disease with spin-echo and gradient-echo sequences. *A.J.R.* 152:159-165.

Carella, F., Grassi, M.P., Savoiardo, M., Contri, P., Rapuzzi, B., and Mangoni, A. 1988. Dystonic-Parkinsonian syndrome after cyanide poisoning: Clinical and MRI findings. *J. Neurol. Neurosurg. Psychiatry* 51:1345-1348.

Chawluk, A. 1999. Neuroimaging of normal brain aging and dementia. *In* Neuroimaging: A Companion to Adams and Victor's Principles of Neurology (J.O. Greenberg, ed.) pp. 301-332. McGraw-Hill, New York.

Choi, I.S. and Cheon, H.Y. 1999. Delayed movement disorders after carbon monoxide poisoning. *Eur. Neurol.* 42:141-144.

Convit, A., De Leon, M.J., Tarshish, C., De Santi, S., Tsui, W., Rusinek, H., and George, A. 1997. Specific hippocampal volume reductions in individuals at risk for Alzheimer's disease. *Neurobiol. Aging* 18:131-138.

Cooper, B. 1994. Health care policy and planning for dementia: An international perspective. *In* Dementia and Normal Aging (F.A. Huppeit and

D.W. O'Conner, eds.) pp. 519-551. Cambridge University Press, Cambridge.

Curran, T. and Lang, A.E. 1994. Parkinsonian syndromes associated with hydrocephalus: Case reports, a review of the literature, and pathophysiological hypotheses. *Mov. Disord.* 9:508-520.

Davis, P.H., Bergeron, C., and McLachlan, D.R. 1985. Atypical presentation of progressive supranuclear palsy. *Ann. Neurol.* 17:337-343.

de Leon, M.J., George, A.E., Stylopoulos, L.A., Smith, G., and Miller, D.C. 1989. Early marker for Alzheimer's disease: The atrophic hippocampus. *Lancet* 2:672-673.

Duguid, J.R., De La Paz, R., and DeGroot, J. 1986. Magnetic resonance imaging of the midbrain in Parkinson's disease. *Ann. Neurol.* 20:744-747.

Evans, D.A., Funkenstein, H.H., Albert, M.S., Scherr, P.A., Cook, N.R., Chown, M.J., Hebert, L.E., Hennekens, C.H., and Taylor, J.O. 1989. Prevalence of Alzheimer's disease in a community population of older persons. Higher than previously reported. *JAMA* 262:2551-2556.

Flicker, C., Ferris, S.H., and Reisberg, B. 1991. Mild cognitive impairment in the elderly: Predictors of dementia. *Neurology* 41:1006-1009.

Friedman, J.H. 1996. Walking-induced Parkinsonism due to presumed idiopathic normal pressure hydrocephalus. *Mov. Disord* 11: 99-101.

Frisoni, G.B., Beltramello, A., Weiss, C., Geroldi, C., Bianchetti, A., and Trabucchi, M. 1996. Linear measures of atrophy in mild Alzheimer disease. *A.J.N.R.* 17:913-923.

Harris, G.J., Pearlson, G.D., Peyser, C.E., Aylward, E.H., Roberts, J., Barta, P.E., Chase, G.A., and Folstein, S.E. 1992. Putamen volume reduction on magnetic resonance imaging exceeds caudate changes in mild Huntington's disease. *Ann. Neurol.* 31:69-75.

Hollister, L.E. and Boutros, N. 1991. Clinical use of CT and MR scans in psychiatric patients. *J. Psychiatry Neurosci.* 16:194-198.

Jack, C.R. Jr., Petersen, R.C., Xu, Y.C., Waring, S.C., O'Brien, P.C., Tangalos, E.G., Smith, G.E., Ivnik, R.J., and Kokmen, E. 1997. Medial temporal atrophy on MRI in normal aging and very mild Alzheimer's disease. *Neurology* 49:786-794.

Jack, C.R. Jr., Petersen, R.C., Xu, Y.C., O'Brien, P.C., Smith, G.E., Ivnik, R.J., Boeve, B.F., Waring, S.C., Tangalos, E.G., and Kokmen, E. 1999. Prediction of AD with MRI-based hippocampal volume in mild cognitive impairment. *Neurology* 52:1397-1403.

Kaye, J.A., Swihart, T., Howieson, D., Dame, A., Moore, M.M., Karnos, T., Camicioli, R., Ball, M., Oken, B., and Sexton, G. 1997. Volume loss of the hippocampus and temporal lobe in healthy elderly persons destined to develop dementia. *Neurology* 48:1297-1304.

Krauss, J.K., Regel, J.P., Droste, D.W., Orszagh, M., Borremans, J.J., and Vach, W. 1997. Movement disorders in adult hydrocephalus. *Mov. Disord.* 12:53-60.

Lang, A.E., Curran, T., Provias, J., and Bergeron, C. 1994. Striatonigral degeneration: Iron deposition in putamen correlates with the slit-like void signal of magnetic resonance imaging. *Can. J. Neurol. Sci.* 21:311-318.

Larson, E.B., Reifler, B.V., Sumi, S.M., Canfield, C.G., and Chinn, N.M. 1986. Diagnostic tests in the evaluation of dementia. A prospective study of 200 elderly outpatients. *Arch. Intern. Med.* 146:1917-1922.

Lee, M.S. and Marsden, C.D. 1994. Neurological sequelae following carbon monoxide poisoning clinical course and outcome according to the clinical types and brain computed tomography scan findings. *Mov. Disord.* 9:550-558.

Ley, C.O. and Gali, F.G. 1983. Parkinsonian syndrome after methanol intoxication. *Eur. Neurol.* 22:405-409.

Messing, B. and Storch, B. 1988. Computer tomography and magnetic resonance imaging in cyanide poisoning. *Eur. Arch. Psychiatry Neurol. Sci.* 237:139-143.

Miodrag, A., Das, T.K., and Shepherd, R.J. 1987. Normal pressure hydrocephalus presenting as Parkinson's syndrome. *Postgrad. Med. J.* 63:113-115.

Olanow, C.W. 1992. Magnetic resonance imaging in Parkinsonism. *Neurol. Clin.* 10:405-420.

Pearson, D.W., Durward, W.F., Fogelman, I., Boyle, I.T., and Beastall, G. 1981. Pseudohypoparathyroidism presenting as severe Parkinsonism. *Postgrad. Med. J.* 57:445-447.

Rosenberg, N.L., Myers, J.A., and Martin, W.R. 1989. Cyanide-induced Parkinsonism: Clinical, MRI, and 6-fluorodopa PET studies. *Neurology* 39:142-144.

Rutledge, J.N., Hilal, S.K., Silver, A.J., Defendini, R., and Fahn, S. 1987. Study of movement disorders and brain iron by MR. *A.J.R.* 149:365-379.

Rydberg, J.N., Riederer, S.J., Rydberg, C.H., and Jack, C.R. 1995. Contrast optimization of fluid-attenuated inversion recovery (FLAIR) imaging. *Magn. Reson. Med.* 34:868-877.

Savoiardo, M., Strada, L., Girotti, F., D'Incerti, L., Sberna, M., Soliveri, P., and Balzarini, L. 1989. MR imaging in progressive supranuclear palsy and Shy-Drager syndrome. *J. Comput. Assist. Tomogr.* 13:555-560.

Savoiardo, M., Strada, L., Girotti, F., Zimmerman, R.A., Grisoli, M., Testa, D., and Petrillo, R. 1990. Olivopontocerebellar atrophy: MR diagnosis and relationship to multisystem atrophy. *Radiology* 174:693-696.

Savoiardo, M., Strada, L., Oliva, D., Girotti, F., and D'Incerti, L. 1991. Abnormal MRI signal in the rigid form of Huntington's disease. *J. Neurol. Neurosurg. Psychiatry* 54:888-891.

Scheltens, P., Leys, D., Barkhof, F., Huglo, D., Weinstein, H.C., Vermersch, P., Kuiper, M., Steinling, M., Wolters, E.C., and Valk, J. 1992. Atrophy of medial temporal lobes on MRI in "prob-

able" Alzheimer's disease and normal ageing: Diagnostic value and neuropsychological correlates. *J. Neurol. Neurosurg. Psychiatry* 55:967-972.

Schoenberg, B.S., Kokmen, E., and Okazaki, H. 1987. Alzheimer's disease and other dementing illnesses in a defined United States population: Incidence rates and clinical features. *Ann. Neurol.* 22:724-729.

Shellock, F.G. and Kanal, E. 1996. Magnetic Resonance Bioeffects, Safety and Patient Management. Lippincott Raven, Philadelphia.

Simmons, J.T., Pastakia, B., Chase, T.N., and Shults, C.W. 1986. Magnetic resonance imaging in Huntington disease. *A.J.N.R.* 7:25-28.

Sohn, Y.H., Jeong, Y., Kim, H.S., Im, J.H., and Kim, J.S. 2000. The brain lesion responsible for Parkinsonism after carbon monoxide poisoning. *Arch. Neurol.* 57:1214-1218.

Soliveri, P., Monza, D., Paridi, D., Radice, D., Grisoli, M., Testa, D., Savoiardo, M., and Girotti, F. 1999. Cognitive and magnetic resonance imaging aspects of corticobasal degeneration and progressive supranuclear palsy. *Neurology* 53:502-507.

Squire, L.R. 1992. Memory and the hippocampus: A synthesis from findings with rats, monkeys, and humans. *Psychol. Rev.* 99:195-231.

Starkstein, S.E., Brandt, J., Bylsma, F., Peyser, C., Folstein, M., and Folstein, S.E. 1992. Neuropsychological correlates of brain atrophy in Huntington's disease: A magnetic resonance imaging study. *Neuroradiology* 34:487-489.

Stern, M.B., Braffman, B.H., Skolnick, B.E., Hurtig, H.I., and Grossman, R.I. 1989. Magnetic resonance imaging in Parkinson's disease and Parkinsonian syndromes. *Neurology* 39:1524-1526.

Verslegers, W., Van den Kerchove, M., Crols, R., De Potter, W., Appel, B., and Lowenthal, A. 1988. Methanol intoxication. Parkinsonism and decreased Met-enkephalin levels due to putaminal necrosis. *Acta. Neurol. Belg.* 88:163-171.

Yock, D.H. 1995. Magnetic Resonance Imaging of CNS Disease—A Teaching File. p. 281. Mosby-Year Book, Inc. (cases 455 and 456).

Zijlmans, J.C., Thijssen, H.O., Vogels, O.J., Kremer, H.P., Poels, P.J., Schoonderwaldt, H.C., Merx, J.L., van 't Hof, M.A., Thien, T., and Horstink, M.W. 1995. MRI in patients with suspected vascular Parkinsonism. *Neurology* 45:2183-2188.

Key References

Shellock and Kanal, 1996. See above.

Covers a number of important patient management issues related to MR imaging, including recommended safety procedures, a list of metallic implants that have been tested for MR compatibility, and a list of other sources on MR safety.

Terry, R.D., Katzman R., and Bick, K.L. 1999. Alzheimer Disease, 2nd Edition. Lippincott Williams & Wilkins, Philadelphia.

A current review of the major aspects of Alzheimer's disease including clinical, epidemiologic, structural, imaging, chemical, genetic, and molecular.

Contributed by Danial K. Hallam
University of Washington
Seattle, Washington

Noriko Salamon-Muramaya
Northwestern University
Chicago, Illinois